Carbohydrate Polymers 80 (2010) 1137–1146

Contents lists available at ScienceDirect

Carbohydrate Polymers

journal homepage: www.elsevier.com/locate/carbpol

Chitosan modified with gadolinium diethylenetriaminepentaacetic acid for magnetic resonance imaging of DNA/chitosan nanoparticles

Vincent Darras [a], Monica Nelea [a], Françoise M. Winnik [b], Michael D. Buschmann [a,c,*]

[a] Department of Chemical Engineering, Ecole Polytechnique, Montreal, Que., Canada
[b] Department of Chemistry and Faculty of Pharmacy, Université de Montreal, Montreal, Que., Canada
[c] Institute of Biomedical Engineering, Ecole Polytechnique, Montreal, Que., Canada

ARTICLE INFO

Article history:
Received 24 November 2009
Received in revised form 13 January 2010
Accepted 14 January 2010
Available online 22 January 2010

Keywords:
Chitosan
DTPA
Gadolinium
Covalent bonding
DNA
pEGFPLuc
Gene delivery
STEM
SEM
ITC
NMR

ABSTRACT

We have prepared chitosan (CH)–gadolinium (Gd) diethylenetriaminepentaacetic acid (DTPA) conjugates that have potential as contrast agents for magnetic resonance imaging. Conjugates were synthesized starting with low molecular weight chitosan (25 kDa and 96% degree of deacetylation (noted DDA)) by covalent linkage of DTPA to chitosan amine groups confirmed by Fourier transform infrared spectroscopy (FTIR). Different DTPA/amine ratios were used to obtain different degrees of DTPA conjugation (10–20%), determined by nuclear magnetic resonance (^{1}H NMR) spectroscopy, a colorimetric assay, and isothermal titration calorimetry (ITC). After preparation of chitosan–DTPA complexes with Gd, polyelectrolyte complexes were assembled with plasmid DNA pEGFPLuc (6367 bp) and investigated using scanning electron microscopy and scanning transmission electron microscopy. Particles were spherical with diameters in the range of 30–150 nm. The presence of gadolinium in the nanoparticles was confirmed by energy dispersive X-ray spectroscopy. Gd was located preferentially in a 2–5 nm wide area surrounding the nanoparticles.

1. Introduction

Magnetic resonance imaging (MRI) contrast agents are used to improve diagnosis of disease (Burstein et al., 2001; Kennedy et al., 1994) and to follow the distribution of therapeutic agents (Canaple et al., 2008). For disease diagnosis, the accumulation of contrast agent within a target tissue or lesion, results in MRI contrast and lesion identification. In the case of therapeutic agents, the MRI contrast material conjugated to the therapeutic agent permits quantification of its biodistribution. An effective approach towards precise targeting of the imaging agent consists of its conjugation to a biopolymer, the "carrier" (Weissleder, Bogdanov, & Papisov, 1995), with inherent affinity for a particular site, or is further conjugated with a moiety which possesses the desired affinity. Typical carrier systems include antibodies, proteins, peptides, polysaccharides, such as dextrans (Rebizak, Schaefer, & Dellacherie, 1997; Wen-Jang Chu, 1995), sodium hyaluronate (Gouin, Grayeb, & Winnik, 2002; Kidd, Mikulis, Turley, Nagy, & Winnik, 1998), other natural polymers (Bligh et al., 1991) as well as synthetic polymers and copolymers as poly-(acrylic acid)-*block*-poly(methyl acrylate) (Turner et al., 2005). Chitosan (CH) is a linear polysaccharide composed of β-(1-4)-linked-2-amino-2-deoxy-D-glucopyranose and 2-acetamido-2-deoxy-D-glucopyranose. It is a non-toxic, biocompatible and biodegradable polymer, obtained via de-*N*-acetylation of chitin, which is the second most abundant polysaccharide after cellulose (Rinaudo, 2006).

The most widely used contrast agents in MRI are complexes of the gadolinium ion (Gd^{3+}) and polyaminocarboxylate ligands, such as diethyltriaminepentaacetic acid (DTPA) (Bligh et al., 1991; Hnatowich et al., 1983; Rebizak et al., 1997). An example is Magnevist®, a contrast agent currently used clinically as an aqueous solution of Gd–DTPA. In the Gd–DTPA complex, the gadolinium is linked by coordination to three nitrogens and five monodentate carboxylate oxygen atoms of the DTPA and to one molecule of water (Caravan, Ellison, McMurry, & Lauffer, 1999). The paramagnetism of the Gd ion results in a significant decrease in water relaxation, generating MRI contrast. There are three types of water molecules surrounding Gd–DTPA: the water far from the complex, with a T_1 value that is not affected by the presence of Gd; water

* Corresponding author. Address: Biomaterials and Cartilage Laboratory, Chemical Engineering Department, Ecole Polytechnique Montreal, P.O. Box 6079, Station Centre-Ville, Montreal, Que., Canada H3C 3A7. Tel.: +1 514 340 4711x4931; fax: +1 514 340 2980.
E-mail address: michael.buschmann@polymtl.ca (M.D. Buschmann).

0144-8617/$ - see front matter © 2010 Elsevier Ltd. All rights reserved.
doi:10.1016/j.carbpol.2010.01.035

within the outer-sphere of the complex which forms hydrogen bonds with the carboxylic moieties of DTPA, and for which Gd induces an increase in relaxivity, $1/T_1$. The third type of water is located within the inner sphere of the Gd–DTPA complex. The paramagnetic Gd^{III} atom exchanges water rapidly within this inner coordination sphere, and thus induces a local relaxation of bulk water protons, providing contrast enhancement (Caravan et al., 1999).

DTPA has been previously bound to chitosan, to provide Gd complexing properties, using two methods: by amide bond formation between chitosan amine bond and DTPA or by electrostatic interactions between NH_3^+ of chitosan and COO^- of DTPA. For covalent binding, DTPA anhydride groups have been reacted with amine moieties of chitosan to form amide bonds (Inoue, Ohto, Yoshizuka, Yamaguchi, & Tanaka, 1997; Inoue, Yoshizuka, & Ohto, 1999; Nagib, Inoue, Yamaguchi, & Tamaru, 1999). In these studies, complexation of chitosan DTPA with metallic ions (Pb II, Fe III, Cu II, Ni II...) was used to obtain water-soluble materials, which bind and remove these ions from water or weak acids such as sulfuric acid.

In the case of ionic binding of chitosan to DTPA (Saha, Ichikawa, & Fukumori, 2006; Shikata, Tokumitsu, Ichikawa, & Fukumori, 2002; Tokumitsu, Ichikawa, & Fukumori, 1999a, 1999b), Ch–DTPA was prepared by emulsion in order to obtain micro- or nano-particles of chitosan loaded with ^{157}Gd complexed with DTPA, as a radiation-producing element for the treatment of tumors. The size of the particles ranged between 400 and 700 nm (Tokumitsu et al., 1999a). Transmission electron microscopy (TEM) suggested that the nanoparticles were not spherical and seemed to be agglomerates consisting of small particles. Chitosan has also been physically mixed with DTPA to give MRI tools in the work of Tan and Zhang (2005). Chitosan particles were prepared by mixing mercaptopropionic acid modified CdSe quantum dots and a commercial gadolinium MRI contrast agent (OMNISCAN®) with chitosan. The quantum dots and MRI contrast agent contained many negative charges which interact with the protonated amine groups of chitosan to form Gd–chitosan–quantum dot nanoparticles with a size of about 100 nm. The main drawback of electrostatic interaction is the possibility of competition by other polyelectrolytes (such as DNA and glycosaminoglycan) which may lead to a release of the complexes DTPA–Gd and a loss of the chitosan label.

More recently the DTPA–Gd complex has been grafted to chitosan (Huang, Huang, Bilgen, & Berkland, 2008) where the Gd–DTPA complex was formed first and then covalently bound to chitosan using a 1-ethyl-3-(3-dimethylaminopropyl)carbodiimide (EDC) and *N*-hydroxylsuccinimide (NHS) mixture. These covalently conjugated Gd–chitosans and physical mixtures of DTPA–Gd and chitosan were then mixed with anionic dextran sulfate to form polyelectrolyte complexes with a size of about 300 nm. These particles were then injected intravascularly in a rat model and found to preferentially accumulate in the kidneys.

In the present study we have synthesized CH–DTPA loaded with gadolinium using an alternative method which enables us to quantify DTPA bound to chitosan using three independent methods. First, we conjugated DTPA to the chitosan with a covalent amide bond and characterized the modified polymer by Fourier transform infrared spectroscopy (FTIR) and ^1H NMR in order to demonstrate the presence of the new bond and to determine the molar ratio of DTPA incorporated to chitosan. We then verified that grafted DTPA can still form complexes with gadolinium by employing colorimetric and ITC (isothermal titration calorimetry) methods which quantify DTPA by forming a complex with Gd in addition to verifying that the structure of DTPA grafted to chitosan is not modified and can still complex Gd. We precisely determined the level of grafting to ascertain that sufficient chitosan amine moieties were retained for subsequent interaction with other polyanions such as DNA (Lavertu, Methot, Tran-Khanh, & Buschmann, 2006). One potential problem was that DTPA bound to chitosan may still have four negatively charged acid functions which could interfere with electrostatic interactions between chitosan and anionic macromolecules. Therefore, we grafted different amounts of Gd–DTPA to chitosan and verified their complexation properties with DNA. Nanoparticles and Gd distribution were then visualized using electron microscopy.

2. Experimental

2.1. Materials

Chitosan (Wako-10, degree of deacetylation (DDA) 85%) was purchased from Wako Chemical Co. 1-ethyl-3-(3-dimethylaminopropyl)carbodiimide (EDC), *N*-hydroxylsuccinimide (NHS), diethylenetriaminepentaacetic acid (DTPA), gadolinium chloride hexahydrate ($GdCl_3{,}6H_2O$), arsenazo III (2,2′-[1,8-dihydroxy-3,6-disulfonaphthylene-2,7-bisazo]-bisbenzenearsonic acid), sodium hydroxide, sodium acetate, deuterium oxide and deuterium chloride, DCl 35 wt% in D_2O were purchased from Aldrich Chemical Co. Glacial acetic acid was purchased from EMD. DOWEX Spectra/Pore membranes (Spectrum) were used for dialysis. Water was deionized using a Milli-Q water purification system (Millipore). Circular DNA plasmid pEGFPLuc (6367 bp) from Clontech Laboratories was used. Plasmid was amplified in DH5α bacteria and purified using the EndoFree Plasmid Mega Kit from Qiagen. Plasmid purity was confirmed with 0.8% agarose gel electrophoresis and by UV spectrophotometry by measuring absorbance at 260 and 280 nm in TE buffer (10 mM Tris–HCl, 1 mM EDTA, pH 8.0). The concentration of pDNA was determined spectrophotometrically (1 A260 nm = 1000 μg/mL). The stock concentration of pEGFPLuc was 1000 μg/mL and the nucleotide molar concentration was determined using an average molar mass of 309 g/mol. Working solutions of DNA plasmids were prepared from stock at 330 μg/mL in double deionized water and stored at −20 °C before use.

2.2. Instrumentation

2.2.1. Gel permeation chromatography analysis

Gel permeation chromatography (GPC) analysis was carried out on a GPC system consisting of an Shimadzu LC-20AD isocratic pump, a Dawn HELEOS II multiangle laser light scattering detector (Wyatt Technology Co.), a Viscostar II (Wyatt Technology Co.), an Optilab rEX interferometric refractometer (Wyatt Technology Co.), and two TSK-GELPW (Tosoh Biosep, G4000 serial number F3373 and G3000 serial number H0012) columns eluted with a pH 4.5 acetic acid (0.3 M)/sodium acetate (0.2 M) buffer (Nguyen, Hisiger, Jolicoeur, Winnik, & Buschmann, 2009a; Nguyen, Winnik, & Buschmann, 2009b). The injection volume was 100 μL, the flow rate was 0.8 mL min^{-1} and the temperature was 25 °C. Solutions for GPC analysis were prepared by dissolving an exact amount of polymer in acetic acid (0.15 M)/sodium acetate (0.1 M) buffer at pH 4.5 to give a concentration of 1.0 mg/mL. The sample solution pH was verified using a Corning pH meter equipped with an Orion electrode. The polymer solutions were kept at room temperature for 1 day under gentle stirring and then filtered through a 0.45 μm membrane prior to the analysis. d*n*/d*c* measurements were carried out using Wyatt manual injector coupled with the Shimadzu LC-20AD pump and the Wyatt Optilab rEX refractometer. The refractive indices of six solutions with different concentration between 0 and 1 mg/mL (0; 0.1; 0.25; 0.5; 0.75 and 1 mg/mL) were recorded for the calculation of d*n*/d*c*.

2.2.2. Nuclear magnetic resonance spectroscopy

Nuclear magnetic resonance (^{1}H NMR) spectroscopy measurements were performed with a 500 MHz NMR spectrometer (Bruker). Solutions of polymer with a concentration of 1% (w/w) were prepared by dissolving 5 mg of chitosan in 1 mL of deuterated water and the pD was adjusted to 6 with DCl and NaOD. Typically, 64 scans were recorded with interscan delays of 6 s and water was used as an internal standard at 60 °C. The degree of deacetylation was established by Lavertu et al. (2003) and calculated using integrals of the peak of proton H1 of deacetylated monomer (noted H1D in Eq. (1)) and the peak of the three protons of acetyl group (HAc) of the non-deacetylated monomer:

$$\mathrm{DDA} = \left(\frac{\mathrm{HID}}{\mathrm{H1D} + (\mathrm{HAc}/3)}\right) \quad (1)$$

2.2.3. Infrared spectrometry

Fourier transmission infrared spectrometry in attenuated total reflection mode (FTIR–ATR) was carried out using a Bruker Vector 55 spectrometer equipped with ATR system MVP from Harrix. UV/vis spectra were measured using a Hewlett–Packard 8452A photodiode array spectrometer.

2.2.4. Isothermal titration calorimetry

Binding isotherms were obtained using a Microcal VP-ITC ultrasensitive titration calorimeter (MicroCal Inc., Northampton, MA) with a cell volume of 1.43 mL. The sample cell was filled with an acetic acid buffered solution of either DTPA (0.45 mM) or CH and CH–DTPA (4.00 mM in glucosamine units) with different amounts of DTPA incorporated. An aqueous acetic acid buffered solution (pH 4.5) of Gd^{3+} (6.50 mM) was placed in a 300 μL syringe that continuously stirred (300 rpm) the cell and injected 25 consecutive aliquots of 5 μL into the cell, delivered over 10 s in intervals of 400 s. Data were collected every 2 s. The measurements were performed at 25 °C. All titrations were carried out three times on freshly prepared solutions to ensure consistency of the data and stability of the solutions. Data analysis was carried out using the Microcal ORIGIN software.

2.2.5. Electron microscopy

Scanning electron microscopy (SEM) investigation was performed on an environmental SEM (ESEM, Quanta 200 FEG, FEI Company Hillsboro, OR) equipped with an energy dispersive X-ray (EDX) spectrometer (Genesis 2000, XMS System 60 with a Sapphire Si/Li Detector from EDAX Inc., Mahwah, NJ). The high vacuum mode of the ESEM microscope was employed for greater resolution and increased contrast for imaging of small features and fine details of complexes and nanoparticles of nanometer size range. High vacuum mode observation parameters were: accelerating voltage = 12.5–20 kV; spot size = 3 and working distance ~5–10 mm. Scanning transmission electron microscopy electron (STEM) investigations were performed on a Jeol JEM-2100F electron microscope with a field emission electron gun (FEG) operating at 200 kV with 0.18 nm point to point resolutions equipped with an EDX spectrometer (EDAX Inc., Mahwah, NJ) with Si/Li detector for chemical microanalysis. In transmission electron microscopy (TEM), the electron beam is transmitted through and interacting with an ultra-thin specimen. In STEM, like in TEM, electrons pass through and interact with the specimen, but the beam is focused to a narrow spot which is scanned over the sample in a raster similarly to SEM. STEM provides complementary information about the chemical composition of the specimens as it produces element-sensitive images with contrast dependent on the *Z*-atomic number using the high angle annular dark field (HAADF) imaging mode. Chemical microanalyses of complexes were performed by EDX in SEM and STEM. Characteristic emission X-ray peaks, specific to each element, appear on the EDX spectra on the *x*-axis and quantified X-rays appear on *y*-axis in counts per second. Spectrometer calibration was performed with standards of copper that has a small number of well-resolved, intense X-ray lines in both low and high energy range. All EDX measurements were performed on at least five sites of similar appearance for a given sample.

2.3. Deacetylation of chitosan

A solution of chitosan (4.0 g, 2.45 mmol of monosaccharide units) in aqueous acetic acid (200 mL, 2 wt%) was added dropwise to aqueous NaOH (100 mL, 50 wt%) at room temperature under magnetic stirring and in an atmosphere of nitrogen. At the end of the addition, the suspension was refluxed for 1 h. It was poured into stirred water (4 L) preheated to 80 °C. The precipitate was decanted, washed five times with water until neutral pH, and separated by filtration. The resulting polymer was purified by dialysis against water for 3 days and isolated by lyophilization (yield 3.2 g, 80%). The DDA determined by ^{1}H NMR was 96%.^{1}H NMR (D_2O): δ 2.36 (3H, H-Ac), δ 3.30 (19H, H-2), δ 3.8–4.3 (101H, H-3 to H-6), δ 5.02 (19H, H-1),

2.4. Preparation of CH–DTPA

Coupling of DTPA with the chitosan was performed using EDC/NHS as coupling agent. A chitosan solution (0.2 g, 1.23 mmol of monosaccharide units) was prepared in 10 mL of deionized water (with 0.8% v/v of HCl 6 M) and the pH was adjusted to 4.7 with NaOH 1 M once the chitosan was dissolved. Ten milliliters of a solution of DTPA (various amount of DTPA (see Table 1) activated with a mixture of NHS ([NHS]/[COOH] = 1.3) and EDC ([EDC]/[COOH] = 1.3) in *N*,*N*,*N*′,*N*′-tetramethylethylenediamine (TEMED) (Aldrich, USA)/HCl buffer solution (pH 4.7) was added to the solution of chitosan and the reaction was left for 72 h at room temperature. The resulting product was purified using a dialysis tube (3500 MWCO) against distilled water for 3 days, followed by lyophilization. For the remaining study, modified chitosan will be called CH–DTPA*X*, where *X* is the % molar ratio of DTPA grafted to chitosan. The targeted molar rations were 10%, 15% and 20% resulting in CH–DTPA10, CH–DTPA15 and CH–DTPA20. Chemicals shifts and integration calculations are summarized in Table 2.

2.5. Colorimetric assays

The colorimetric assay of the level of DTPA incorporation in CH–DTPA is based on the large bathochromic shift of the absorbance of arsenazo III in the presence of transition metals, such as Gd^{3+}, due to the formation of a stable complex (Savvin, 1961). The free dye has a strong visible absorption at 548 nm. It absorbs at 660 nm when complexed with heavy metals. The colorimetric assay provides the degree of conjugation of DTPA on CH–DTPA via a protocol based on the addition of an excess Gd^{3+} to a solution of CH–DTPA, and the quantitative analysis of the excess of gadolin-

Table 1
Experimental conditions of CH–DTPA synthesis as described in Section 2.4.

Name	CH–DTPA10	CH–DTPA15	CH–DTPA20
n_{NH_2} (mmol)	1.18	1.18	1.18
n_{DTPA} (mmol)	0.120	0.178	0.242
[DTPA]/[NH_2]	0.10	0.15	0.20
n_{EDC} (mmol)	0.782	1.17	1.56
n_{NHS} (mmol)	0.782	1.17	1.56
Yield (% w/w)[a]	82	75	80

[a] Yield is the ratio of mass of CH–DPTA/CH × 100.

Table 2
Chemical shifts in ^{1}H NMR (D_2O) for the protons of the three CH–DTPA.

	Hac	H-2 and H-D	H-B	H-C	H-3 to H-6 and H-A	H-1
CH–DTPA10	δ 2.36	δ 3.32–3.37	δ 3.59	δ 3.69	δ 3.8–4.4	δ 5.05
	3H	31H	5H	10H	137H	22H
CH–DTPA15	δ 2.36	δ 3.30–3.45	δ 3.60	δ 3.70	δ 3.8–4.4	δ 5.08
	3H	43H	8H	18H	182H	26H
CH–DTPA20	δ 2.35	δ 3.32–3.37	δ 3.59	δ 3.70	δ 3.8–4.4	δ 5.05
	3H	47H	11H	23H	178H	26H

ium detected as its complex with arsenazo III (λ_{max} = 660 nm). A calibration curve was obtained by measuring the absorbance at 660 nm of a series of standard solutions of the arsenazo III/Gd^{3+} complex prepared by mixing stock solutions of $GdCl_3$ (0.2 mM) and arsenazo III (0.2 mM) in water. Excess of $GdCl_3$,$6H_2O$ (10 mg) was added to a solution of CH–DTPA (20 mg in 13 mL water) and the mixture was subjected to ultrafiltration using a Diaflo system mounted with YM-10 membranes (Amicon, Beverly, MA, molecular weight cutoff: 10 kDa). The polymer solution was washed with 10 mL of water, and four samples of the filtrate (10.0 mL each) were collected during ultrafiltration. The concentration of Gd^{3+} in the filtrate was analyzed as follows: an aliquot of the filtrate (500 μL) was added to the arsenazo III stock solution (1.0 mL). The solution was made up to exactly 10 mL. The absorbance of the solution was measured at 660 nm. The arsenazo III/Gd^{3+} concentration of the sample was determined using the calibration curve. This value corresponds to the excess Gd^{3+} added to the CH–DTPA solution analyzed. The concentration of polymer bound with DTPA was obtained by subtracting the excess Gd^{3+} determined by colorimetry from the total amount of Gd^{3+} added to the sample.

2.6. Formation of plasmid chitosan–Gd nanoparticles and sample preparation for electron microscopy

CH–DTPA20 was dissolved in deionized water overnight on a rotary mixer. 1.0 mL of a 0.1 M $GdCl_3$ solution was added and after 5 min, the mixture was subjected to ultrafiltration using a Diaflo system mounted with YM-10 membranes (Amicon, Beverly, MA, molecular weight cutoff: 10 kDa). The polymer solution was washed with 50 mL of water, and the filtrate was collected during ultrafiltration. The level of gadolinium incorporated was determined by a colorimetric assay of the filtrate (see Section 2.5: colorimetric assays for details of titration) and the CH–DTPA20–Gd solution was recovered from the ultracentrifugation cell and freeze dried for 3 days.

CH–DTPA20–Gd was dissolved overnight on a rotary mixer at 0.5% (w/v) in hydrochloric acid using a glucosamine:HCl ratio of 1:1. Chitosan solutions were then diluted with deionized water to reach the desired amine (deacetylated groups) to phosphate ratio when 50 μL of chitosan was mixed with 50 μL of pDNA, the latter always at a concentration of 330 mg/mL in endotoxin-free TE. The final amine–phosphate (N:P) ratio was 5:1.

Specimens for SEM were prepared on freshly-cleaved muscovite mica surfaces by dropping from solutions, and then dried and gold-sputtered (Agar Manual Sputter Coater, Marivac Inc., Montreal, QC). TEM and STEM specimens were prepared by immersing the carbon-covered copper grids in nanoparticle solutions for 10 s and then left to dry in air. In order to increase the image contrast and better distinguish the background around particles, a slight uranyl acetate (0.1% v/v) stain was performed on some nanoparticles of plasmid DNA complexed with chitosan that had not been conjugated with Gd–DTPA. The 0.1% uranyl acetate staining was performed by immersing the grid with the dried specimen for 2 s and then left to dry in air.

3. Results and discussion

The conjugation of DTPA to chitosan was carried out using an almost fully deacetylated chitosan, obtained by deacetylating a commercial chitosan with a nominal DDA of 85%, using a previously described procedure (Zhang, Oh, Allen, & Kumacheva, 2004). The resulting DDA was 96% as determined by ^{1}H NMR. Fig. 1 illustrates the synthesis of CH–DTPA in which EDC and NHS were used as the activation agents with details of reaction conditions presented in Table 1. EDC induces the activation of carboxylic groups to give *O*-acyl urea ester groups (Nakajima & Ikada, 1995), and the reaction of these activated carboxylic groups with the amino group-containing materials forms the amide bond. Based on this concept, activated carboxylic groups of DTPA were formed using EDC in the presence of the nucleophile NHS in order to enhance the reaction as adapted from a method described by Chung et al. (2002). The yield of the reaction is summarized in Table 1 according to:

$$\text{yield } (\%_{m/m}) = \frac{\text{CH—DTPA final mass}}{\text{CH starting mass}} \times 100 \quad (2)$$

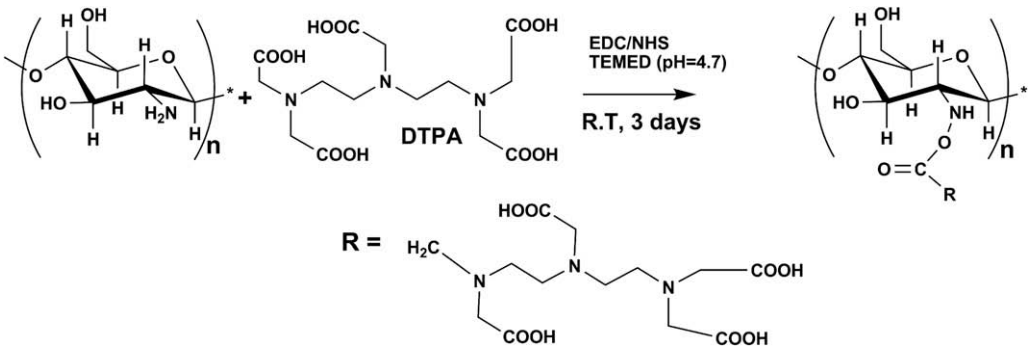

Fig. 1. Synthesis of CH–DTPA (right structure) from chitosan (CH) and diethylenetriaminepentaacetic acid (DTPA) using 1-ethyl-3-(3-dimethylaminopropyl)carbodiimide (EDC) and *N*-hydroxylsuccinimide (NHS).

For the three products, the yield ranges from 75% to 85% where the loss of product may be due to the purification step.

3.1. Gel permeation chromatography analysis

All CH–DTPA samples were characterized by gel permeation chromatography (Table 3). Before analysis, the d*n*/d*c* of different modified chitosans was calculated. The average d*n*/d*c* was 0.163, and did not change with an increase of DTPA content, and was lower than pure chitosan which has a d*n*/d*c* of 0.218. The DTPA carrying five carboxylic groups could potentially react with amine functions of several chitosan chains and induce crosslinking of the chitosan which would then be characterized by a large increase of average molecular weight or insolubility. However, CH–DTPA with different amounts of DTPA had similar number average molecular weights. The calculated molecular weight was higher than the starting chitosan due to the DTPA grafting. The grafting of an anionic molecule to chitosan, especially the diethylenetriaminepentaacetic acid with multiple acid functions, will affect the shape of the macromolecules and therefore its elution properties. The addition of anionic groups to chitosan may also screen the positive charge of the amine and as a result the chitosan might be more compact resulting in a shorter elution time. The absence of an increase of the molecular weight or a second peak at smaller retention time confirms the absence of a crosslinking reaction between multiple chitosan chains and DTPA which could be possible since DTPA carries five carboxylic groups which could bind with the amine functions of different chitosan chains and significantly increase molecular weight. Intrachain binding is nonetheless possible and was not detectable with gel permeation chromatography.

Table 3
Molecular mass by GPC, level of DTPA incorporation by NMR, ITC and colorimetry for CH–DTPA with different amounts of grafted DTPA.

	M_n (g mol^{-1})	M_w (g mol^{-1})	M_w/M_n	mol% DTPA (NMR)	mol% DTPA (UV)	mol% DTPA (ITC)
CH	17,000	40,000	2.35	0	0	0
CH–DTPA10	27,000	40,000	1.48	11 ± 2	9 ± 2	10 ± 1
CH–DTPA15	28,000	55,000	1.96	15 ± 2	11 ± 2	12 ± 1
CH–DTPA20	28,000	51,000	1.82	21 ± 2	16 ± 2	18 ± 1

3.2. FTIR analysis

The grafting of DTPA to chitosan is a reaction of an acid to an amine resulting in the formation of an amide bond which can be observed in IR. The IR spectra of DTPA (Fig. 2) presents bands at 1730, 1696 and 1630 cm^{-1}, corresponding to the C=O bending of COOH in the form of monomer, dimer and carboxylate, respectively. The band at 1391 cm^{-1} can also be attributed to the COO$^-$ function and has been observed in other CH–DTPA compounds where DTPA and CH are linked by electrostatic interactions (Saha et al., 2006). For chitosan, the large band between 1100 and 1000 cm^{-1} is due to vibration of C—O bond of alcohol and to —C—O—C— vibration of the monosaccharide unit, in agreement with the values are reported in the literature (Justi, Favere, Laranjeira, Neves, & Casellato, 2005). In the case of CH–DTPA samples, the band of C=O bond of DTPA at 1620 cm^{-1} and the band of C—O and C—O—C are observed at 1620 cm^{-1} and between 1100 and 1000 cm^{-1}, respectively, but a shoulder appears at 1530 cm^{-1} and is not observed in the physical mixture of CH and DTPA. This shoulder can be attributed to amide II band (Chung et al., 2002) and had also been observed by Huang et al. when they grafted DTPA–Gd complex to chitosan (Huang et al., 2008). Its presence suggests that DTPA is covalently attached to the chitosan backbone by an amide bond.

3.3. NMR analysis

^{1}H NMR was used to confirm IR results and calculate the level of DTPA incorporated in chitosan. All CH–DTPA samples were characterized by NMR spectroscopy and the spectra were similar with peaks at the same chemical shifts. The only difference was for the integrals of the DTPA peaks, which were proportional to DTPA content. In Fig. 3, we showed the spectrum of chitosan and CH–DTPA15. The signal at 5.08 ppm was attributed to the resonance of anomeric protons of *N*-glucosamine units and the signal at 2.35 ppm to the three protons of non-deacetylated monosaccharide units (representing 4% of the units). Signals at 4.12, 3.7 and 3.6 ppm were assigned to protons A, C and B of DTPA, respectively. The signal between 3.3 and 3.4 ppm was an overlap of the chitosan proton binding the carbon 2 of chitosan and D protons of DTPA. An increase of 0.05 ppm of the chemical shift of anomeric proton can

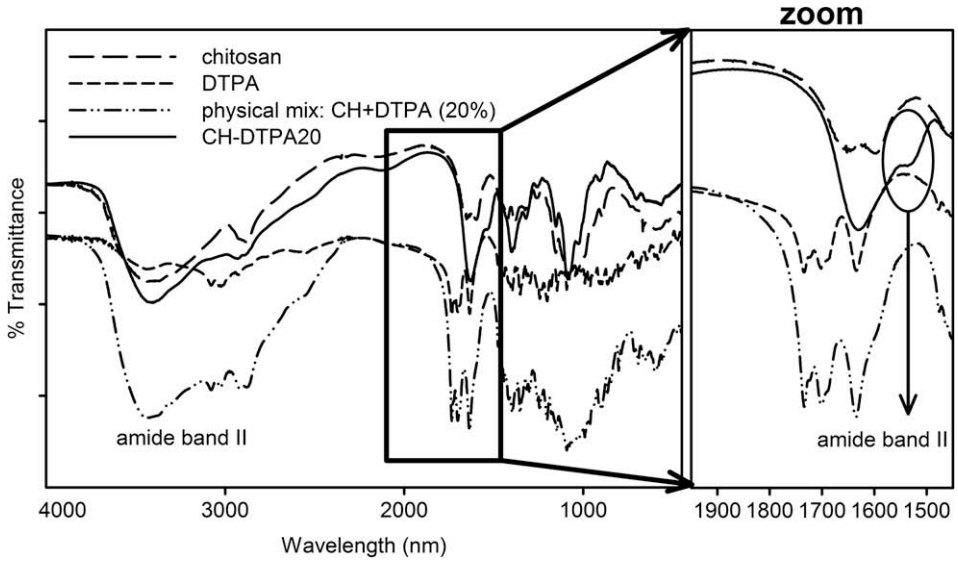

Fig. 2. FTIR spectra of deacetylated chitosan, DTPA, a physical mixture of chitosan and DTPA and a modified chitosan with 20% (mol/mol) DTPA. The shoulder at 1530 cm^{-1} indicates covalent bonding between by an amide bond between CH and DTPA.

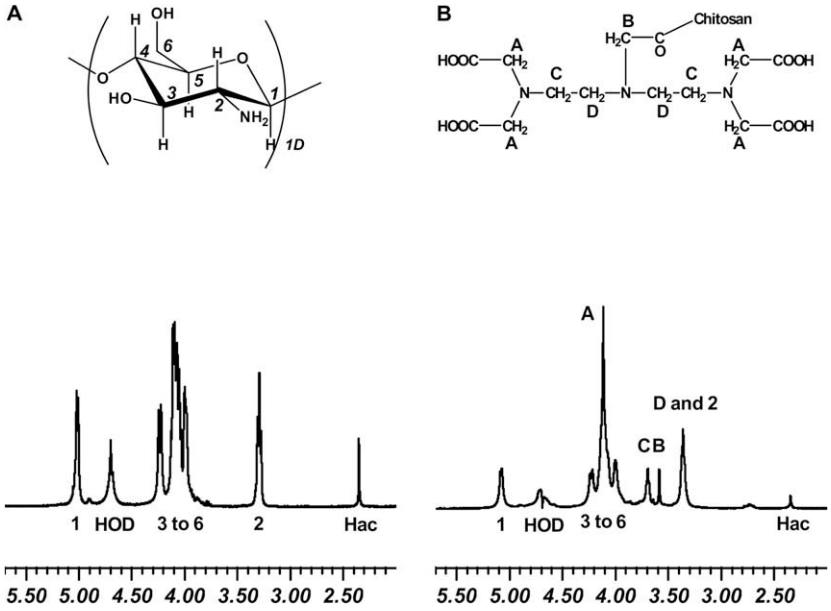

Fig. 3. ^{1}H NMR spectra of (A) CH and (B) CH–DTPA15 in D_2O (pH 6 at 60 °C), showing peak assignments. The molar ratio of DTPA grafted to chitosan was calculated using the integration of peak B for DTPA and peaks 1 and Hac for CH.

be attributed to a change of the chemical environment near this proton and we might assume that this change was due to the covalent binding between DTPA and chitosan.

The DTPA content (degree of substitution or DS) was calculated using the integrals of the proton peak B of the DTPA and proton H1D and HAc of chitosan:

$$\mathrm{DS} = \left(\frac{\mathrm{B}/2}{\mathrm{H1D} + \mathrm{HAc}/3}\right) \quad (3)$$

The DS values for all the samples are summarized in Table 3. In all cases, the amount calculated by NMR is the same as the amount of DTPA added at the beginning and suggests that the coupling reaction is complete and quantitative. However, DTPA has five acid functions and thus five p*Ka* (10.48; 8.60; 4.28; 2.60; 2.00) (Deal, Motekaitis, Martell, & Welch, 1996). Thus dialysis against double deionized water may allow electrostatic interactions to persist between chitosan which has positive charge and negative carboxylic function of DTPA. In order to confirm covalent bonding, dialysis was done against dilute sodium hydroxide at pH 9 for 3 days followed by dialysis against pure water until pH was neutral. At pH 9 CH–DTPA was still soluble, a good indication of covalent bonding between DTPA and chitosan, since the amine function of glucosamine function is not protonated at this pH (Lavertu, Filion, & Buschmann, 2008). This lack of positive charge would enable the elimination of uncovalently bound DTPA from the samples. Amounts calculated after this purification were the same as those obtained by dialysis against water, confirming covalent bonding between chitosan and DTPA. For the following studies, dialysis against water was done in order to control the amount of ionic species in the chitosan, which may affect the stability of complexes with DNA. With FTIR presented above, we also showed covalent bonding of DTPA to chitosan and with NMR we additionally verified that the amount of DTPA added to chitosan is the same as that bound to chitosan.

3.4. Colorimetric analysis

The ability of DTPA to complex to gadolinium was assessed by quantitative analysis with colorimetric assays and ITC. In order to verify that the chitosan backbone does not complex Gd^{3+} ions, chitosan without DTPA was also titrated. The results are summarized in Table 3. It is apparent that the chitosan backbone does not complex with Gd^{3+} since the excess of Gd^{3+} is totally recovered by ultrafiltration. In the case of CH–DTPA, the difference between the amount of gadolinium added and recovered is via its complexation with DTPA. The amount of DTPA conjugated to chitosan for all samples reported (Table 3) is similar to that found by NMR with the difference between NMR and the colorimetric method (1% or 2%) attributed to experimental error. The ability of DTPA to strongly complex gadolinium depends on the geometry of the DTPA molecule (Caravan et al., 1999). Therefore, we may conclude that the covalently bound DTPA still complexes with gadolinium and the percentage found by colorimetry similar to that found by ^{1}H NMR. Thus we may assume that DTPA is attached by one arm of the molecule and there is no intramolecular reaction with any other amine function close to the DTPA and its remaining acid functions.

3.5. Isothermal titration calorimetry analysis

Isothermal titration calorimetry (ITC) allows direct measurement of the amount of DTPA grafted to chitosan which can complex with gadolinium. The quantitative determination of the number of DTPA groups linked to a polymer backbone relies on the precise measurement of the number of binding sites offered to Gd^{3+} by the conjugated polymer. We carried out titrations of Gd^{3+} in solutions of various CH–DTPA samples, as well as in a solution of unmodified CH. In Fig. 4, the experimental titration curves are shown for Gd^{3+} in buffer (a), in a buffered solution of CH (b), and in a buffered solution of CH–DTPA15 (c); long with Fig. 5 the corresponding binding curves obtained by integration of each peak of the CH–DTPA and subtraction of the dilution enthalpy. We note that dilution of Gd^{3+} into the buffer is affected by the presence of CH (compare traces a and b in Fig. 4). The presence of exothermic peaks instead of endothermic peak for the case of chitosan in buffer may be due to an exchange of counter ion in the area of NH_3^+ function of chitosan, since we add Cl^- in the cell and we can assume replacement of AcO^- counterions by Cl^-. In the case of CH–DTPA15, this phenomenon is still present but small (~1 μcal/s) in comparison with to the complexation of Gd III by DTPA (5 μcal/

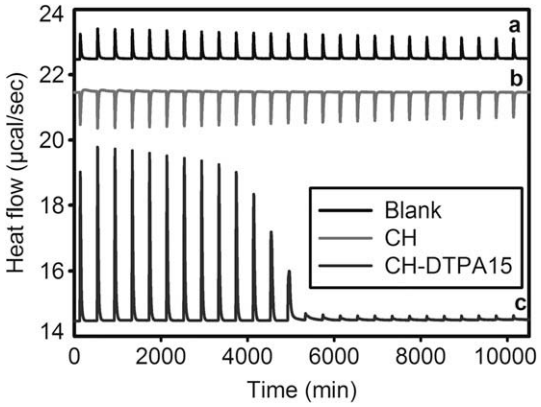

Fig. 4. Isothermal titration calorimetry curves of Gd^{3+} into aqueous polymer solutions at 25 °C and pH 4.2 in acetic acid buffer. Calorimetric traces (heat flow vs. time) for (a) the blank (acetic acid buffer), (b) CH and (c) CH–DTPA15. The heat flow of the blank and CH is negligible compared to those of CH–DTPA.

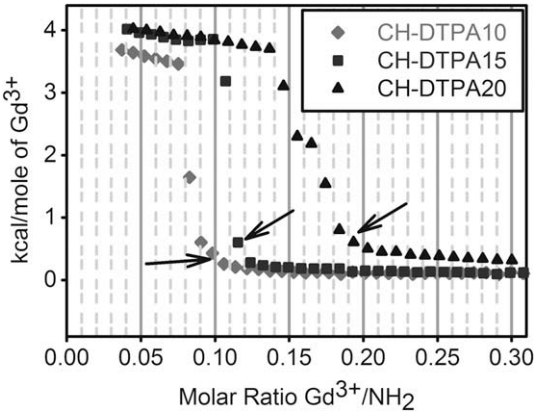

Fig. 5. Titration curves of Gd^{3+} into aqueous polymer solutions at 25 °C and pH 4.2. Reaction enthalpy (obtained by integrating the peaks of the curve c in Fig. 3) vs. Gd^{3+}/*N*-glucosamine unit ratio (mol/mol). Assuming one Gd^{3+} ion binds to one DTPA molecule, the amount of DTPA is calculated when the plateau is attained as indicated by arrows.

s). In the binding experiments, the injections produce strong endothermic signals associated with the formation of the DTPA–Gd complex until saturation. The enthalpy of binding, $\delta H_{binding}$, is around 4 kcal/mol of Gd^{3+} and it slightly decreased after the first injections. Then, as the Gd III concentration reaches saturation corresponding to a DTPA/Gd^{3+} molar ratio of 1 (which is proportionate to the molar ratio Gd^{3+}/NH_2 equal to 0.10 in the CH–DTPA15), the heat released decreases rapidly and at higher concentrations of Gd III, approaches 0. The suggested upper limit of detection of this method for measuring a binding constant is around $\sim 10^9$ L mol^{-1} (Freire, Mayorga, & Straume, 1990) and the constant for the association of DTPA and Gd value found in the literature is 2.9×10^{22} L mol^{-1} (Caravan et al., 1999). Therefore we assumed that the complexation was complete when the $\delta H_{binding}$ reached a constant value. The resulting degrees of substitution for different amounts of DTPA incorporated in chitosan are summarized in Table 3. If we assume that exactly one gadolinium ion binds to 1 DTPA unit, the titration indicates that 12 mol% of the amino groups of CH bear a DTPA unit in the CH–DTPA15 sample. The DTPA–Gd binding constant was too high to be quantified by ITC. The degrees of substitution found by ITC are similar to those determined by colorimetric assays and by ^{1}H NMR and the differences (up to 2%) were within experimental error. This direct method confirms the ability of the grafted DTPA to complex gadolinium with efficiency is near 100%.

3.6. Electron microscopy investigation

The ability of conjugated and non-conjugated chitosan to form complexes with plasmid DNA was investigated using electron microscopy. Particles formed with plasmid pEGFLuc and unconjugated chitosan have globular shape with diameter sizes in the range of 30–100 nm and average diameter of 60 nm, as observed in SEM (Fig. 6A). First solutions of Gd-containing nanoparticles were prepared by chitosan conjugated with Gd–DTPA, with DTPA of 10 and 15 mol%. Since at these DTPA percentage amounts gadolinium was undetectable in particles by EDX in SEM, the percentage of DTPA was increased. At 20 mol% DTPA, EDX peaks characteristic of Gd could be discriminated from background. Mixing plasmid pEGFLuc with CH–DTPA20–Gd produces slightly larger globular particles than with unconjugated chitosan with diameters in the range of 30–230 nm (Fig. 6B) and an average diameter of 100 nm. Thus, the presence of DTPA and gadolinium seem to influence complexation leading to the formation of particles with larger size. Our results are compatible with results of galactose-modified chitosan–pEGFP–N1 particles prepared at the same N:P ratio (Kim, Park, Nah, Choi, & Cho, 2004) where particles are reported as spherical with about 100 nm average diameter. EDX–SEM microanalysis of a CH–DTPA20–Gd/pEGFLuc particle confirmed qualitatively the presence of Gd^{3+} in specimens as shown by two small peaks characteristic to Gd^{3+} in Fig. 6C. The most prominent X-ray contributors in EDX spectra came from the mica substrate (K, Si,

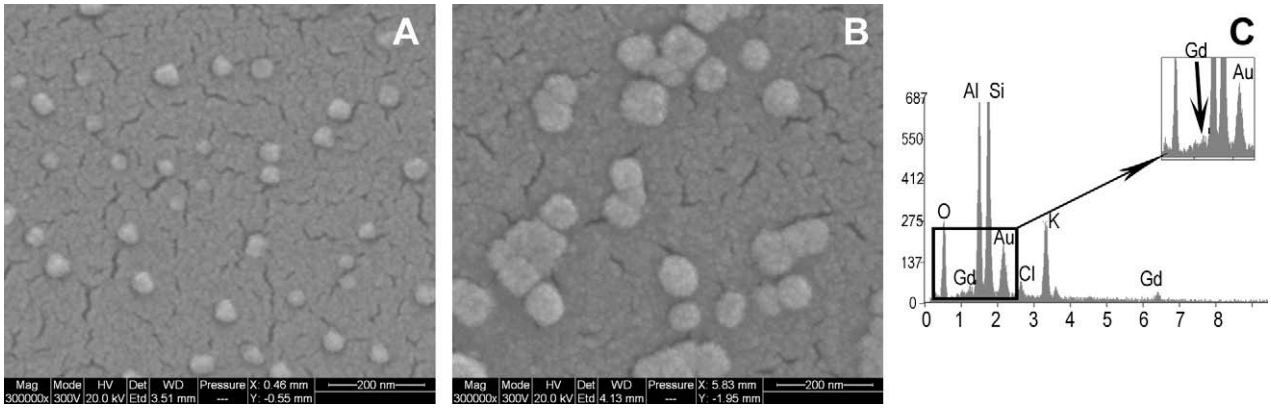

Fig. 6. ESEM images of chitosan–pEGFPLuc nanoparticles (A) chitosan without DTPA and Gd (B) particles with CH–DTPA20–Gd and (C) EDX analyses of one particle. Particles formed with unconjugated chitosan have an average diameter of 60 nm (Fig. 5A) while 100 nm was found when using chitosan–DTPA20–Gd (Fig. 5B).

Al, and O) as electrons at this energy penetrate the specimen to depth of tens of micrometers.

Exploiting the STEM capability of being sensitive to atomic number, we pursued with STEM imaging to identify and localize Gd in the particle. STEM-HAADF (high angle annular dark field) is a technique that allows us to observe electron-beam-sensitive samples with reduced electron-beam damage, which is critical in the case of polymeric nanoparticles since the interaction with the TEM electron beam can produce severe structural changes in a short time. The sizes of the particles with and without the presence of DTPA20–Gd as measured in STEM are in the range of 30–200 nm, close to SEM results. In the case of unconjugated CH–pEGFLuc bright (Fig. 7A and B) contrast patterns were obtained over the whole particle surface. When not stained with uranyl acetate, particles appear with a uniformly-distributed white color over the whole particle surface with a somewhat fuzzy edge-contour and a background (space around the particle) that is grey (Fig. 7A). This image pattern is typical for particles made of organic material since differences of atomic numbers of constitutive elements are very low, and images without *Z*-contrast are produced (Fig. 7A). After uranyl acetate staining, a sufficient contrast was produced to visualize details of space around particles (Fig. 7B) where linear white structures that may represent uncomplexed (free) chitosan have retained uranyl acetate ions. A certain substructure of the chitosan–DNA particle is distinguishable with a randomly bright/less-bright pattern generated after penetration of stain through the organic material of the particle, while the particle edge is more clearly defined (Fig. 7B). In the case of particles prepared with chitosan conjugated with DTPA20–Gd without uranyl staining, high resolution images (Fig. 7C and D) display brighter features at the level of the edges of the particle as compared to the darker or less-brighter central regions of particles (arrows in Fig. 7C and D). The width of the bright mantle contour surrounding the particle is 2–5 nm (dash delineating marks in Fig. 7D). Bright features with dot-like structure of 1–2 nm diameter visible in the space between nanoparticles in Fig. 7C and D are likely CH–DTPA20–Gd that has remained free after complexation and not bound to the nanoparticle. Since samples of particles made of chitosan conjugated with Gd were not uranyl acetate stained, the only contrast in micrographs of Fig. 7C and D is generated by Gd that is the marker for chitosan localization. Gadolinium is a heavy element with atomic number Gd (64) well distanced from atomic numbers of other (light) elements in the specimens, i.e., C (6), N (7), and O (8). In STEM the signal generating the image is from electrons undergoing scattering events at high angles with intensity directly proportional to the square of the element atomic number (Browning et al., 2000). Since image contrast is generated by differences in these signal intensities, and there is the large atomic number gap between Gd and either C, N or O, we found high contrast patterns as in the micrographs of Fig. 7C and D, providing a direct visual indication of gadolinium labelled chitosan localized close to the particle surface within a shell of 2–5 nm width. Fig. 8 shows an EDX spectrum performed in STEM of CH–DTPA20–Gd particles where the presence of Gd in the particle was qualitatively proven.

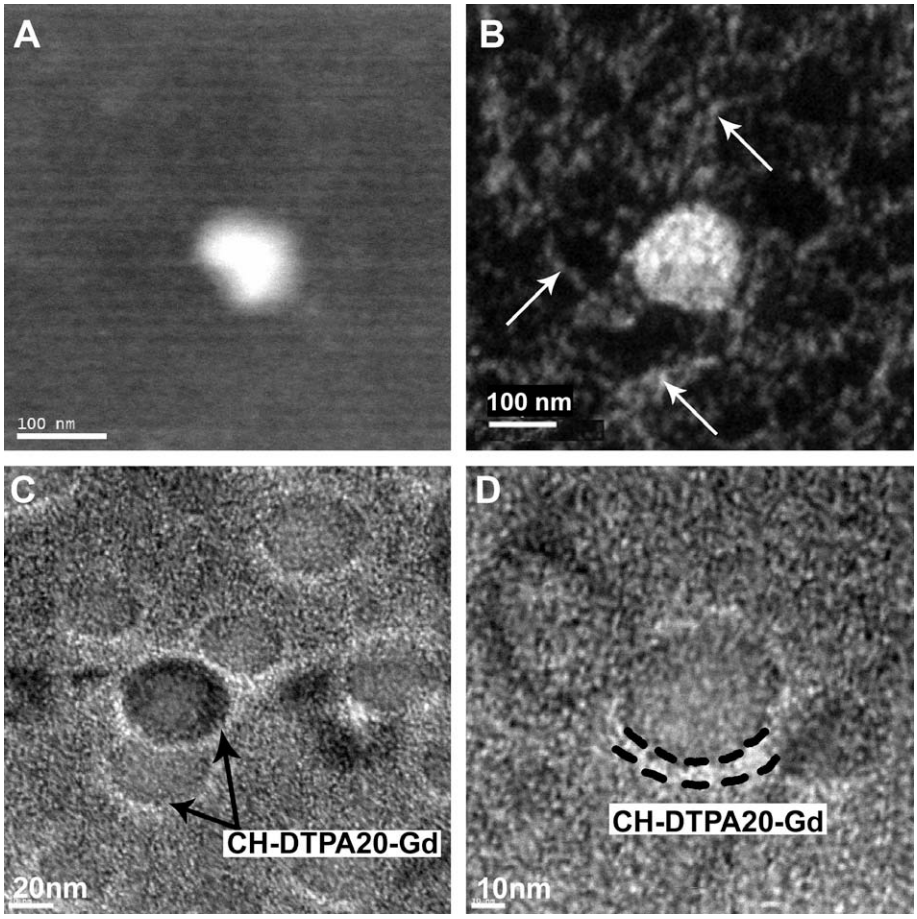

Fig. 7. STEM images of microstructure of CH–pEGFPLuc particles without uranyl acetate staining (A) with slight uranyl acetate staining (B) and of CH–DTPA20–Gd–pEGFLuc particles without uranyl acetate staining (C and D). The average diameter of particles with and without DTPA20–Gd is about 80 nm. Staining with uranyl acetate renders free chitosan observable in B (white arrows). The large atomic number gap in Gd labelled particles, Gd (64), C (6), N (7), and O (8) produces a high contrast pattern in (C and D) with direct visual indication of gadolinium localized close to the particle surface within a shell of 2–5 nm width (arrows and dashed line in C and D).

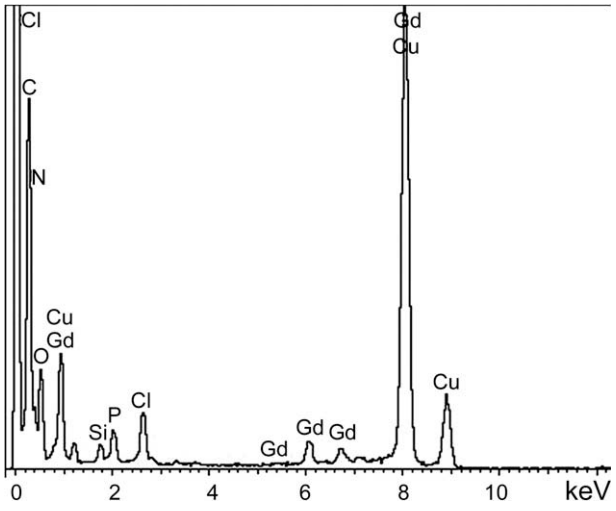

Fig. 8. EDX analyses of one particle with CH–DTPA20–Gd performed in STEM at 20 kV. The EDX spectrum performed on particles formed with CH–DTPA20–Gd demonstrate the presence of Gd in the particle.

4. Conclusion

In contrast to previous works where gadolinium was first complexed to DTPA and then grafted or physical mixed to polymer, we adopted a strategy of first grafting the chelating agent, DTPA, and then complexing gadolinium to permit characterization of the efficiency of each step. Different percentages (10–20 mol%) of DTPA were conjugated to chitosan with EDC and NHS. The covalent linkage between chitosan and DTPA was confirmed by infrared spectroscopy and the GPC measurements found no crosslinking between DPTA and multiple chitosan chains. The lack of initial complexation to gadolinium allowed us to determine the amount of DTPA conjugated by ^{1}H NMR which was similar to the amount added with a yield between 75% and 85%. The ability of grafted DTPA to bind gadolinium was then assessed using colorimetry and ITC. The initial grafting of DTPA to chitosan did not affect the efficiency of DTPA complex with Gd. This efficiency was nearly 100% since the amount of DTPA calculated by 1H NMR was similar in all cases to that determined by colorimetric studies and confirmed by ITC. We finally verified that the presence of DTPA and gadolinium did not adversely affect the ability of chitosan to form polyelectrolyte complexes with the DNA plasmid pEGFPLuc. At the ratio N:P = 5, the particles as seen in electron microscopy had an average diameter of 100 nm, slightly larger than the particles formed with chitosan without DTPA–Gd (60 nm in diameter) STEM imaging revealed for the first time in such systems that the conjugated Gd was present in a 2–5 nm thick mantle at the periphery of these spherical nanocomplexes of chitosan and pDNA.

Acknowledgements

The work was supported by Biosyntech Canada Inc., the Natural Sciences and Engineering Council of Canada and the Canadian Institutes of Health Research.

References

Bligh, S. W. A., Harding, C. T., Sadler, P. J., Bulman, R. A., Bydder, G. M., Pennock, J. M., et al. (1991). Use of paramagnetic chelated metal derivatives of polysaccharides and spin-labeled polysaccharides as contrast agents in magnetic resonance imaging. *Magnetic Resonance in Medicine, 17*(2), 516–532.

Browning, N. D., James, E. M., Kishida, K., Arslan, I., Buban, J. P., Zaborac, J. A., et al. (2000). Scanning transmission electron microscopy. An experimental tool for atomic scale interface science. *Reviews on Advanced Materials Science, 1*(1), 1–26.

Burstein, D., Velyvis, J., Scott, K. T., Stock, K. W., Kim, Y. J., Jaramillo, D., et al. (2001). Protocol issues for delayed Gd(DTPA)(2−)-enhanced MRI: (dGEMRIC) for clinical evaluation of articular cartilage. *Magnetic Resonance in Medicine, 45*(1), 36–41.

Canaple, L., Beuf, O., Armenean, M., Hasserodt, J., Samarut, J., & Janier, M. (2008). Fast screening of paramagnetic molecules in zebrafish embryos by MRI. *NMR in Biomedicine, 21*(2), 129–137.

Caravan, P., Ellison, J. J., McMurry, T. J., & Lauffer, R. B. (1999). Gadolinium(III) chelates as MRI contrast agents: Structure, dynamics, and applications. *Chemical Reviews, 99*(9), 2293–2352.

Chung, T. W., Yang, J., Akaike, T., Cho, K. Y., Nah, J. W., Kim, S. I., et al. (2002). Preparation of alginate/galactosylated chitosan scaffold for hepatocyte attachment. *Biomaterials, 23*(14), 2827–2834.

Deal, K. A., Motekaitis, R. J., Martell, A. E., & Welch, M. J. (1996). Evaluation of the stability and animal biodistribution of gadolinium(III) benzylamine-derivatized diethylenetriaminepentaacetic acid. *Journal of Medicinal Chemistry, 39*(16), 3096–3106.

Freire, E., Mayorga, O. L., & Straume, M. (1990). Isothermal titration calorimetry. *Analytical Chemistry, 62*(18), A950–A959.

Gouin, S., Grayeb, V. V., & Winnik, F. M. (2002). Gadolinium diethylenetriaminepentaacetic acid hyaluran conjugates: Preparation, properties and applications. *Macromolecular Symposia, 186*, 105–110.

Hnatowich, D. J., Layne, W. W., Childs, R. L., Lanteigne, D., Davis, M. A., Griffin, T. W., et al. (1983). Radioactive labeling of antibody: A simple and efficient method. *Science, 220*(4597), 613–615.

Huang, M., Huang, Z. L., Bilgen, M., & Berkland, C. (2008). Magnetic resonance imaging of contrast-enhanced polyelectrolyte complexes. *Nanomedicine: Nanotechnology, Biology and Medicine, 4*(1), 30–40.

Inoue, K., Ohto, K., Yoshizuka, K., Yamaguchi, T., & Tanaka, T. (1997). Adsorption of lead(II) ion on complexane types of chemically modified chitosan. *Bulletin of the Chemical Society of Japan, 70*(10), 2443–2447.

Inoue, K., Yoshizuka, K., & Ohto, K. (1999). Adsorptive separation of some metal ions by complexing agent types of chemically modified chitosan. *Analytica Chimica Acta, 388*(1–2), 209–218.

Justi, K. C., Favere, V. T., Laranjeira, M. C. M., Neves, A., & Casellato, A. (2005). Synthesis and characterization of modified chitosan through immobilization of complexing agents. *Macromolecular Symposia, 229*, 203–207.

Kennedy, S. D., Szczepaniak, L. S., Gibson, S. L., Hilf, R., Foster, T. H., & Bryant, R. G. (1994). Quantitative MRI of Gd–DTPA uptake in tumors – Response to photodynamic therapy. *Magnetic Resonance in Medicine, 31*(3), 292–301.

Kidd, G. H., Mikulis, D. J., Turley, E. A., Nagy, J. I., & Winnik, F. M. (1998). Hayluronan-based imaging agents. US Patent Application 60/083, 311.

Kim, T. H., Park, I. K., Nah, J. W., Choi, Y. J., & Cho, C. S. (2004). Galactosylated chitosan/DNA nanoparticles prepared using water-soluble chitosan as a gene carrier. *Biomaterials, 25*(17), 3783–3792.

Lavertu, M., Filion, D., & Buschmann, M. D. (2008). Heat-induced transfer of protons from chitosan to glycerol phosphate produces chitosan precipitation and gelation. *Biomacromolecules, 9*(2), 640–650.

Lavertu, M., Methot, S., Tran-Khanh, N., & Buschmann, M. D. (2006). High efficiency gene transfer using chitosan/DNA nanoparticles with specific combinations of molecular weight and degree of deacetylation. *Biomaterials, 27*(27), 4815–4824.

Lavertu, M., Xia, Z., Serreqi, A. N., Berrada, M., Rodrigues, A., Wang, D., et al. (2003). A validated H-1 NMR method for the determination of the degree of deacetylation of chitosan. *Journal of Pharmaceutical and Biomedical Analysis, 32*(6), 1149–1158.

Nagib, S., Inoue, K., Yamaguchi, T., & Tamaru, T. (1999). Recovery of Ni from a large excess of Al generated from spent hydrodesulfurization catalyst using picolylamine type chelating resin and complexane types of chemically modified chitosan. *Hydrometallurgy, 51*(1), 73–85.

Nakajima, N., & Ikada, Y. (1995). Mechanism of amide formation by carbodiimide for bioconjugation in aqueous-media. *Bioconjugate Chemistry, 6*(1), 123–130.

Nguyen, S., Hisiger, S., Jolicoeur, M., Winnik, F. M., & Buschmann, M. D. (2009a). Fractionation and characterization of chitosan by analytical SEC and H-1 NMR after semi-preparative SEC. *Carbohydrate Polymers, 75*(4), 636–645.

Nguyen, S., Winnik, F. M., & Buschmann, M. D. (2009b). Improved reproducibility in the determination of the molecular weight of chitosan by analytical size exclusion chromatography. *Carbohydrate Polymers, 75*(3), 528–533.

Rebizak, R., Schaefer, M., & Dellacherie, E. (1997). Polymeric conjugates of Gd^{3+}-diethylenetriaminepentaacetic acid and dextran. 1. Synthesis, characterization, and paramagnetic properties. *Bioconjugate Chemistry, 8*(4), 605–610.

Rinaudo, M. (2006). Chitin and chitosan: Properties and applications. *Progress in Polymer Science, 31*(7), 603–632.

Saha, T. K., Ichikawa, H., & Fukumori, Y. (2006). Gadolinium diethylenetriaminopentaacetic acid-loaded chitosan microspheres for gadolinium neutron-capture therapy. *Carbohydrate Research, 341*(17), 2835–2841.

Savvin, S. B. (1961). Analytical use of arsenazo III: Determination of thorium, zirconium, uranium and rare earth elements. *Talanta, 8*(9), 673–685.

Shikata, F., Tokumitsu, H., Ichikawa, H., & Fukumori, Y. (2002). In vitro cellular accumulation of gadolinium incorporated into chitosan nanoparticles designed for neutron-capture therapy of cancer. *European Journal of Pharmaceutics and Biopharmaceutics, 53*(1), 57–63.

Tan, W. B., & Zhang, Y. (2005). Multifunctional quantum-dot-based magnetic chitosan nanobeads. *Advanced Materials, 17*, 2375–2380.

Tokumitsu, H., Ichikawa, H., & Fukumori, Y. (1999a). Chitosan–gadopentetic acid complex nanoparticles for gadolinium neutron-capture therapy of cancer: Preparation by novel emulsion-droplet coalescence technique and characterization. *Pharmaceutical Research, 16*(12), 1830–1835.

Tokumitsu, H., Ichikawa, H., Fukumori, Y., & Block, L. H. (1999b). Preparation of gadopentetic acid-loaded chitosan microparticles for gadolinium neutron-capture therapy of cancer by a novel emulsion-droplet coalescence technique. *Chemical & Pharmaceutical Bulletin, 47*(6), 838–842.

Turner, J. L., Pan, D., Plummer, R., Chen, Z., Whittaker, A. K., & Wooley, K. L. (2005). Synthesis of gadolinium-labeled shell-crosslinked nanoparticles for magnetic resonance imaging applications. *Advanced Functional Materials, 15*(8), 1248–1254.

Weissleder, R., Bogdanov, A. A. J., & Papisov, M. (1995). *Handbook of targeted delivery of imaging agents*. Boca Raton, FL: CRC Press.

Wen-Jang Chu, G. A. E. (1995). Gadolinium and dysprosium chelates of DTPA–amide–dextran: Synthesis, H-1 NMR relaxivity, and induced Na-23 NMR shift. *NMR in Biomedicine, 8*(4), 159–163.

Zhang, H., Oh, M., Allen, C., & Kumacheva, E. (2004). Monodisperse chitosan nanoparticles for mucosal drug delivery. *Biomacromolecules, 5*(6), 2461–2468.